Tyrosine Side-Chain Functionalities at Distinct Positions Determine the Chirooptical Properties and Supramolecular Structures of Pentameric Oligothiophenes

Marcus Bäck,[a] Robert Selegård,[b] Yogesh Todarwal,[c] Sofie Nyström,[a] Patrick Norman,[c] Mathieu Linares,[d, e, f] Per Hammarström,[a] Mikael Lindgren,[a, g] and K. Peter R. Nilsson*[a]

Control over the photophysical properties and molecular organization of π-conjugated oligothiophenes is essential to their use in organic electronics. Herein we synthesized and characterized a variety of anionic pentameric oligothiophenes with different substitution patterns of L- or D-tyrosine at distinct positions along the thiophene backbone. Spectroscopic, microscopic, and theoretical studies of L- or D-tyrosine substituted pentameric oligothiophene conjugates revealed the formation of optically active π-stacked self-assembled aggregates under acid conditions. The distinct photophysical characteristics, as well as the supramolecular structures of the assemblies, were highly influenced by the positioning of the L- or D-tyrosine moieties along the thiophene backbone. Overall, the obtained results clearly demonstrate how fundamental changes in the position of the enantiomeric side-chain functionalities greatly affect the optical properties as well as the architecture of the self-assembled supramolecular structures.

1. Introduction

Self-assembled chiral materials comprised of conjugated poly- and oligothiophenes (CPs and COs) have been extensively studied due to their potential for being utilized in optoelectronic devices, biosensors, and as artificial enzymes.[1–11] CPs with an optically active substituent in the 3-position normally display optical activity in the π–π* transition region when the polymer chains are forming supramolecular, π-stacked self-assembled aggregates in a poor solvent or at low temperature.[5,12–15] Furthermore, when mixing optically inactive CPs and COs with small chiral molecules or synthetic peptides, an induced single-chain chirality that reflects the stereochemistry of the chiral guest can be obtained.[9–11,16–20] An analogous single-chain induced chirality have also been observed for CPs having optically active zwitter-ionic side chain functionalities, as well as in CPs functionalized with L- or D-amino acid side chains.[21,22] For the latter, the chirality of the side chain was manifested in the conformation of the polymer backbone, giving rise to right-handed or left-handed helical forms of the polythiophene chains with induced circular dichroism (ICD) patterns of the two polymers that were mirror images.[22]

ICD has also been reported for chemically defined oligothiophenes having chiral substituents at distinct positions along the thiophene backbone.[23–27] The chiral moieties can be introduced in the β-positions of the thiophene moieties[23] or at the terminal α-positions of the oligothiophene backbone.[24–27] For α,α'-linked oligothiophenes with five, six, or seven thiophene rings, with penta(ethyleneoxide) substituents attached via ester links at the terminal α-positions, the sign of the aggregation induced Cotton effect was dependent on the position of the chiral substituent as well as the length of the oligothiophene sequence.[24] Similarly, tetrameric oligothiophenes displayed opposite Cotton effects depending on the introduction of suitable D-(+)- or L-(−)-mannosidic building blocks linked to the terminal α-positions.[25] An analogous effect was also obtained when mixing α-sexithiophene with distinct polysaccharides.[28] Lately, it was also shown that oligiothiophene-proline hybrids display specific self-assembly behaviour in an aqueous environment by forming chiral superstructures, whose helicity and Cotton effect were controlled by the

[a] Dr. M. Bäck, Dr. S. Nyström, Prof. P. Hammarström, Prof. M. Lindgren, Prof. K. P. R. Nilsson
Division of Chemistry, Department of Physics, Chemistry and Biology, Linköping University,
581 83 Linköpin (Sweden)
E-mail: peter.r.nilsson@liu.se
[b] Dr. R. Selegård
Division of Biophysics and Bioengineering, Department of Physics, Chemistry and Biology, Linköping University,
581 83 Linköping (Sweden)
[c] Y. Todarwal, Prof. P. Norman
Department of Theoretical Chemistry and Biology, KTH Royal Institute of Technology, SE-106 91 Stockholm (Sweden)
[d] Dr. M. Linares
Laboratory of Organic Electronics, ITN, Linköping University, SE-601 74 Norrköping, Sweden
[e] Dr. M. Linares
Scientific Visualization group, ITN, Linköping University, SE-601 74 Norrköping, Sweden
[f] Dr. M. Linares
Swedish e-Science Research Center (SeRC), Linköping University,
581 83 Linköping (Sweden)
[g] Prof. M. Lindgren
Department of Physics, Norwegian University of Science and Technology, Gløshaugen
7491 Trondheim (Norway)

Supporting information for this article is available on the WWW under https://doi.org/10.1002/open.202000144

configuration of the amino acid moiety.[26] Thus, a variety of studies have shown that enantiomeric substitutions can be utilized to tune the optical properties as well as the structural organization of oligothiophenes. However, the differences in optical behaviour and self-assembly between oligothiophenes having the same enantiomeric substituents in the β-positions of the thiophene moieties or at the terminal α-positions of the oligothiophene backbone have not been examined.

Herein we report the synthesis of a set of novel anionic pentameric oligothiophenes having L-tyrosine or D-tyrosine introduced at distinct positions along the conjugated backbone (Figure 1). Amino acid residues were introduced at the β-position of distinct thiophene moieties or at the terminal α-positions of the oligothiophene backbone and the effects of the structural modifications were investigated by comparing the photo-physical characteristics and self-assembling properties of the chiral oligothiophenes. The obtained results revealed how alterations in the position of the enantiomeric moiety have a large impact on the oligothiophenes optical properties as well as the molecular architecture of the self-assembled structures.

2. Results and Discussion

2.1. Synthesis of Pentameric Oligothiophenes with Tyrosine Side Chain Functionalities

To achieve a library of chiroptical pentameric oligothiophenes with tyrosine substituents in the β-positions of distinct thiophene moieties or at the terminal α-positions of the oligothiophene backbone (Figure 1), the previously reported achiral oligothiophenes, penta hydrogen thiophene acetic acid (p-HTAA) and penta formyl thiophene acetic acid methylester (p-FTAM), as well as a trimeric building block, compound **2**, were selected as templates (Supporting Information, SI Scheme S1).[29,30] The two enantiomers, p-HTA-L-Tyr and p-HTA-D-Tyr, were afforded by addition of L- or D-tyrosine to the carboxylate functionalities in the β-positions of p-HTAA[29] through an amide forming reaction using hexafluorophosphate azabenzotriazole tetramethyl uronium (HATU) followed by removal of protecting groups to have anionic side chain functionalities. A similar synthetic route was applied for p-FTAM,[29] to achieve the two enantiomers, p-FTAA-L-Tyr and p-FTAA-D-Tyr, having tyrosine functionalities at the terminal α-positions of the pentameric thiophene backbone, as well as acetate functionalities in the β-positions of thiophene number 2 and 4. The third pair of enantiomers, p-FTA-L-Tyr and p-FTA-D-Tyr, was generated by hydrolysis of the carboxylate functionalities in the β-positions of **2**[29] followed by applying the HATU

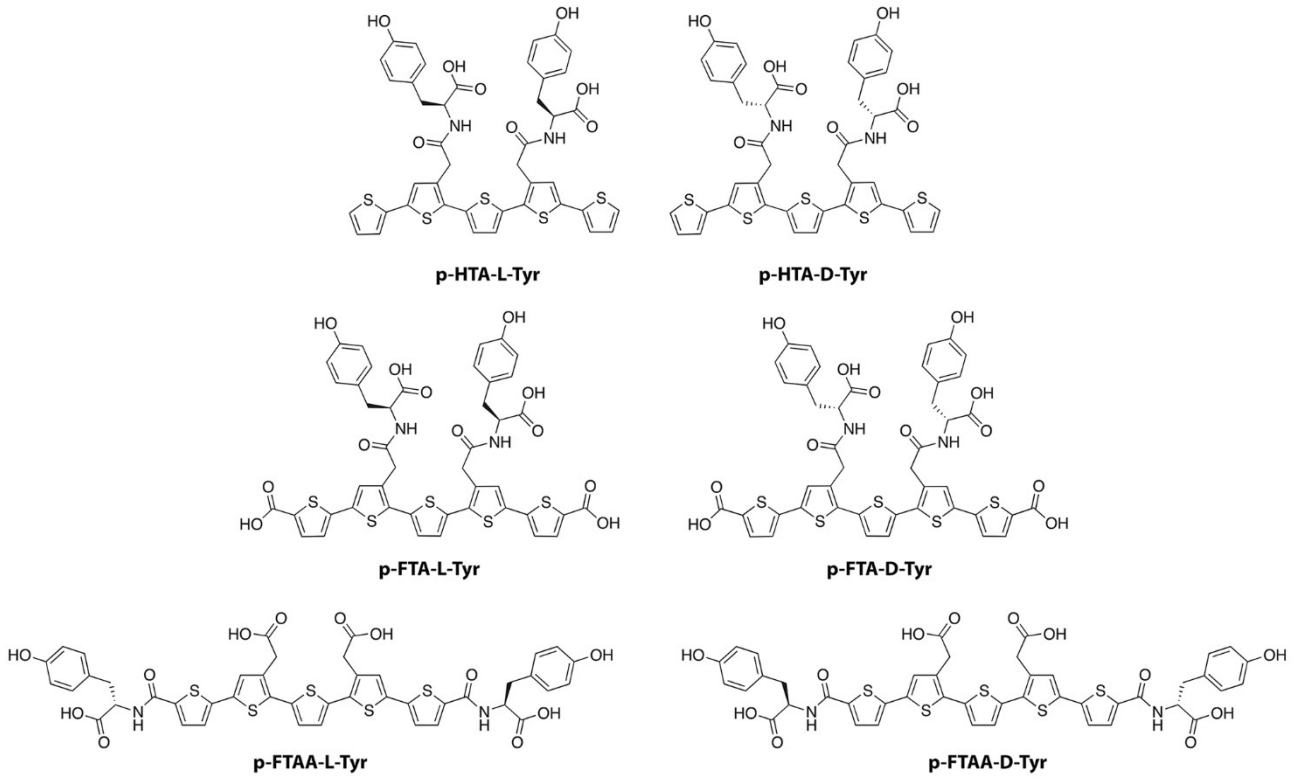

Figure 1. Chemical structures of the fully protonated pentameric oligothiophenes having L- (left panel) or D-tyrosine (right panel) side-chain functionalities at distinct positions along the thiophene backbone. In acidic conditions (pH 1.7) all the carboxyl groups of the oligothiophenes should predominantly be protonated, whereas in alkaline conditions (pH 12.3), the carboxyl groups, as well as the phenylic hydroxy groups should be deprotonated.

mediated amide forming reaction to add L- or D-tyrosine to generate the brominated trimer **3**. To yield pentameric oligothiophenes having tyrosine functionalities in the β-positions of thiophene number 2 and 4, as well as carboxylate functionalities at the terminal α-positions of the pentameric thiophene backbone, the addition of 5-carboxy-2-thienylboronic acid to **3** was afforded by palladium-mediated Suzuki-Miyaura cross coupling followed by removal of protecting groups. As a part of removing protective groups or in additional final step, all the pentameric ligands were converted to the sodium salt using sodium hydroxide (SI, Scheme S1).

2.2. Absorption and Emission Characteristics

Next the photo-physical characteristics of the tyrosine-functionalized oligothiophenes dissolved in 20 mM HCl or 20 mM NaOH (pH 12.3) were evaluated (Figure 2). These acidic and basic conditions were selected, since earlier studies have shown that pH-induced conformational changes of the thiophene backbone can be afforded for both anionic oligo- and polythiophenes.[29–33] In addition, in 20 mM HCl (pH 1.7) all the carboxyl groups of the oligothiophenes should predominantly be protonated, whereas in 20 mM NaOH (pH 12.3), the carboxyl groups, as well as the phenolic hydroxy groups should be deprotonated. In 20 mM NaOH, p-HTA-L-Tyr and p-HTA-D-Tyr, displayed similar absorption spectra with a maximum at 400 nm, as well as comparable emission maxima around 520 nm (Figure 2A). These photophysical characteristics are similar to ones reported for other anionic pentameric oligothiophenes in alkaline conditions, suggesting that the absorption- and emission spectra from the ligands in 20 mM NaOH originates from fully dissolved single oligothiophene chains or tiny clusters of chains.[29–33] Both dyes also showed analogous optical characteristic in 20 mM HCl, but the absorption spectra showed a red-shift, as well as two additional peaks around 330 nm and 275 nm, compared to the spectra in alkaline conditions. A red-shift of the spectra were also observed for the emission and is most likely associated with a planarization of the backbone that are induced upon protonation of the carboxyl groups.[21,34–37] In addition, the emission intensity decreased with almost two orders of magnitude, suggesting an aggregation of adjacent oligothiophene molecules (SI, Figure S1).[13–15,21] p-FTA-L-Tyr and p-FTA-D-Tyr showed an equivalent photophysical behavior as their counterparts lacking the α-terminal carboxyl groups (Figure 2B and Figure S1). However, in 20 mM HCL, the emission spectra were strikingly more red-shifted with emission maxima at 640 nm, suggesting that alternative aggregates are formed due to the α-terminal carboxyl groups.

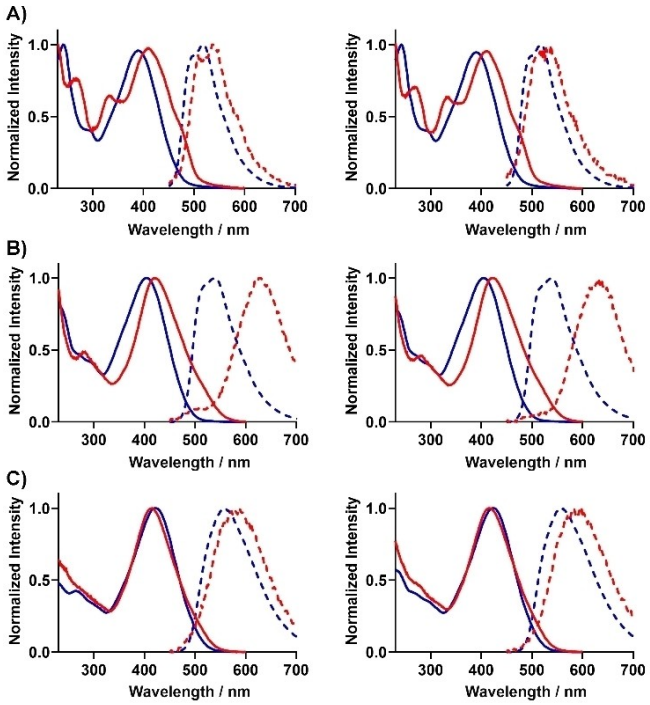

Figure 2. Photophysical characteristics of the pentameric oligothiophenes. **A)** Normalized absorption- (line) and emission spectra (dotted line) of 50 μM p-HTA-L-Tyr (left panel) or 50 μM p-HTA-D-Tyr (right panel) in 20 mM NaOH (blue) or 20 mM HCl (red). **B)** Normalized absorption- (line) and emission spectra (dotted line) of 50 μM p-FTA-L-Tyr (left panel) or 50 μM p-FTA-D-Tyr (right panel) in 20 mM NaOH (blue) or 20 mM HCl (red). **C)** Normalized absorption- (line) and emission spectra (dotted line) of 50 μM p-FTAA-L-Tyr (left panel) or 50 μM p-FTAA-D-Tyr (right panel) in 20 mM NaOH (blue) or 20 mM HCl (red).

The third pair of enantiomers, p-FTAA-L-Tyr and p-FTAA-D-Tyr displayed comparable absorption maxima in acidic or basic conditions, but a small shoulder at longer wavelengths could be observed in the absorption spectra in 20 mM HCl (Figure 2C). Furthermore, in acidic conditions the emission spectra were red-shifted, and a decrease of the emission intensity was also observed (Figure 2B and Figure S1). Hence, similar to the other pentameric oligothiophenes, p-FTAA-L-Tyr and p-FTAA-D-Tyr seem to form π-stacked self-assembled aggregates upon protonation of the carboxyl groups, whereas fully dissolved single oligothiphene chains are obtained in alkaline conditions. However, from a photophysical perspective, these aggregates seem to be different compared to the other pairs of enantiomers, suggesting that the swapping of the tyrosine side chain functionality from the β-positions of distinct thiophene moieties to the terminal α-positions of the oligothiophene backbone is influencing the morphology of the aggregates. For instance, the addition of tyrosine to the terminal α-positions might induce some steric effects that generate an alternative aggregate formation.

Overall, the absorption- and emission measurements confirmed that the changes in the positions of the enantiomeric tyrosine side chain functionalities have a substantial impact on the oligothiophenes optical properties, as well as that all of the ligands form different types of aggregates in acidic conditions. Depending on their photophysical behaviour, molecular assemblies of oligo- and polythiophenes have been classified as J-aggregates or H-aggregates.[38–41] In general, the formation of J-aggregates creates a red-shift of the main absorption peaks compare to the monomer in solution, whereas the opposite, a blue-shift is observed for H-aggregate formation. Thus, according to the absorption data (Figure 2), p-HTA-L-Tyr, p-HTA-D-Tyr,

p-FTA-L-Tyr and p-FTA-D-Tyr presumably form J-aggregates in acidic conditions. However, there can be several sources of spectral red-shifts, such as intrachain planarization,[21,34–37] and it was recently suggested that an anionic pentameric oligothiophene, penta formyl thiophene acetic acid (p-FTAA), regardless of a pH-induced red-shift of the absorption forms H-aggregates in acidic conditions.[32,33] Similar to p-FTA-L-Tyr and p-FTA-D-Tyr, p-FTAA displayed a decreased and striking red-shifted emission (640 nm) at pH 2,[33] suggesting that this pair of enantiomers might also forms H-aggregates in acidic environment.

In order to study the emission characteristics in more detail, time-correlated single photon counting (TC-SPC) measurements were carried out to determine the decay times of the enantiomeric variants. These experiments were performed at lower concentrations (5 μM) of the oligothiophenes to ensure that inner filter effects or quenching from intermolecular energy transfer processes were minimized. As judged from the absorption spectra (Figure 2) a laser diode operating at 403 nm was appropriate for the excitation of all oligothiophenes. Although the decays all were close to mono-exponential, the decays were analyzed allowing two decay times. By using these two decay times and the amplitude weights, an intensity averaged decay time, τ_{ave}, was calculated. The L- and D-enantiomers of p-HTA-Tyr showed averaged decay times around 110 to 140 ns in acidic condition (20 mM HCl), whereas τ_{ave} increased to about 300 ps under basic conditions (20 mM NaOH) (Figure 3A). In contrast, p-FTA-L-Tyr and p-FTA-D-Tyr displayed longer average decay times in 20 mM HCl (τ_{ave} around 500 ps) compared to decay times achieved in alkaline conditions (τ_{ave} around 270 ps) (Figure 3B). Thus, these two pairs of enantiomers displayed opposite pH-induced effects on the average decay times. It is noted that p-FTA-L-Tyr and p-FTA-D-Tyr, for which the life-time increased, also showed a large red-shift of the emission in acidic conditions (Figure 2B). Thus, the alignment in the p-FTA-L-Tyr and p-FTA-D-Tyr aggregates seems to have more efficiently planarized molecular moieties. The third pair of enantiomers, p-FTAA-L-Tyr and p-FTAA-D-Tyr, showed longer average decay times in 20 mM NaOH (τ_{ave} around 460 to 490 ps) compared to acidic conditions (τ_{ave} around 230 to 245 ps) (Figure 3C). For all pairs of enantiomers, the apparent decay time along with the analyzed decay times were essentially the same within experimental uncertainty when comparing L- and D-type enantiomers. Nevertheless, the three pairs of enantiomers displayed specific averaged decay times in 20 mM HCl or 20 mM NaOH, verifying that the emission characteristics of the oligothiophenes are highly dependent on the location of the tyrosine side chain functionalities, as well as the charge of the anionic groups.

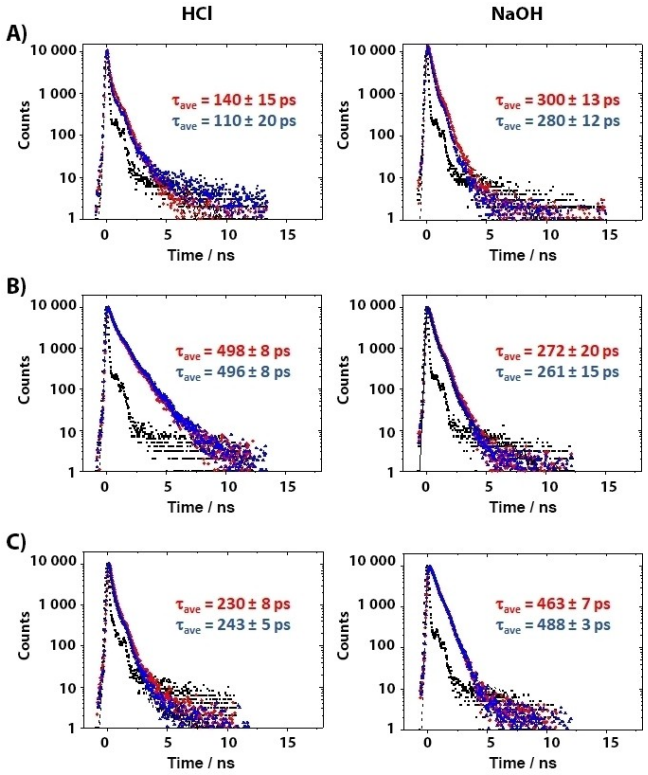

Figure 3. TC-SPC decays of the three pairs of enantiomers, A) p-HTA-L-Tyr (blue) and p-HTA-D-Tyr (red). **B)** p-FTA-L-Tyr (blue) and p-FTA-D-Tyr (red). **C)** p-FTAA-L-Tyr (blue) and p-FTAA-D-tyr (red). All the measurements were recorded for 5 μM ligand in 20 mM HCl (left panel) or in 20 mM NaOH (right panel) with excitation at 403 nm and the emission was recorded at the respective emission maximum (A: 500 nm (HCl) and 485 nm (NaOH); B: 625 nm (HCl) and 530 nm (NaOH); C: 570 nm (HCl) and 540 nm (NaOH)). All decays could be analysed with two decay times with parameters as in the insets showing the intensity average lifetime.

2.3. Induced Circular Dichroism

To investigate the optical activity in the π–π* transition region of the pentameric oligothiophenes, we next performed circular dichroism (CD) measurements in 20 mM HCl or 20 mM NaOH. In acidic conditions, all three ligands displayed a strong split-type ICD in the π–π* transition region, whereas only minor signals lacking the bisignate Cotton effect were observed in alkaline conditions (Figure 4 and SI, Figure S2). Similar to earlier observations of chiral oligo- and polythiophenes,[5,12–16,24–27] this indicates that the strong ICDs may be associated with π-stacked chiral aggregation of the oligothiophenes. This indication is also supported by the already discussed red-shifts in absorption spectra and decreased emission intensities under acidic condition (Figure 2 and SI, Figure S1). The strongest and most pronounced ICD was obtained for the p-HTA-Tyr enantiomers (Figure 4A), whereas the two other pairs of enantiomers displayed similar but less intense ICD patterns (Figure 4B–C). As previously reported for optical active polythiophenes,[13,15] the ICD pattern resembled the first derivative of the absorption for the respective ligand (SI, Figure S3). All ligands functionalized with L-tyrosine showed a positive Cotton effect at lower energy and a negative Cotton effect at higher energy, whereas the ICD patterns of the ligands functionalized with D-tyrosine were mirror images compared to the corresponding enantiomers (Figure 4). Hence, the altered chirality of the tyrosine side chain functionality is influencing the helical packing of the thiophene backbone. Similar ICD patterns have also been observed for zwitter-ionic polythiophenes having L- or D-serine in the β-positions, although the ICDs in these polythiophenes were a

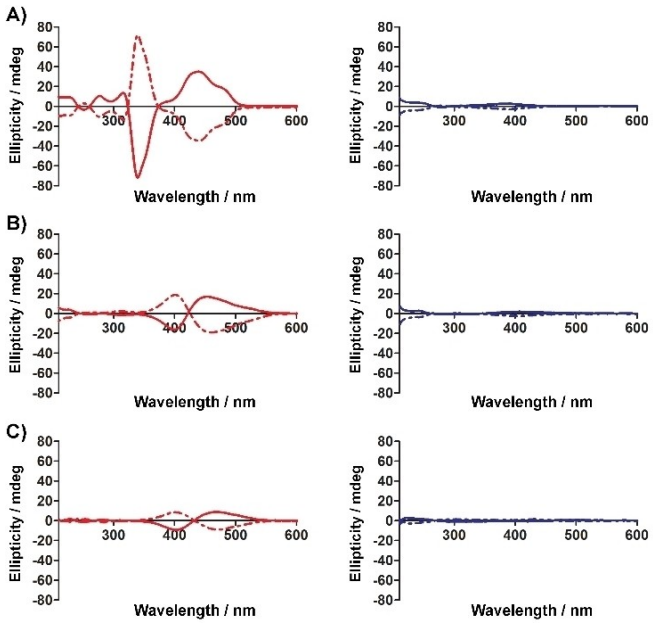

Figure 4. Circular dichroism spectra (CD) of the pentameric oligothiophenes. A) CD spectra of 50 μM p-HTA-L-Tyr (line) or 50 μM p-HTA-D-Tyr (dotted line) in 20 mM HCl (left panel) or 20 mM NaOH (right panel). **B)** CD spectra of 50 μM p-FTA-L-Tyr (line) or 50 μM p-FTA-D-Tyr (dotted line) in 20 mM HCl (left panel) or 20 mM NaOH (right panel). **C)** CD spectra of 50 μM p-FTAA-L-Tyr (line) or 50 μM p-FTAA-D-Tyr (dotted line) in 20 mM HCl (left panel) or 20 mM NaOH (right panel).

result of main-chain chirality instead of aggregation.[21] Interestingly, in 20 mM NaOH mirror images of the CD spectra in the UV region (210–260 nm) were also observed for all pairs of enantiomers, verifying that the chirality of tyrosine side chain is preserved (SI, Figure S2). In addition, when mixing equal amounts of the D- or L-form of the respective oligothiophenes in 20 mM NaOH, racemic mixture with no CD-signal was obtained (SI, Figure S2).

To get a microscopic insight into the origin of the ICD, we performed a computational study by combining classical force-field molecular dynamics (MD) and quantum-mechanical spectrum simulations (see the SI for further details). As target system, we adopted the protonated D-form of p-HTA-Tyr, since this ligand showed the largest ICD (Figure 4A).

We first investigated the ICD at the single-molecule level, assessing how a chiral twist-deformation of the conjugated backbone induces a CD signal in a model system. We constructed a series of models of *cis*-pentathiophene with varying negative dihedral angles between the thiophene groups, a conformation referred to as MMMM (M for minus). The molecular structures were either fully relaxed or the dihedral angles were locked at specific values while the rest of the molecule was relaxed. The CD spectra of these systems as obtained by time-dependent density functional theory (TD-DFT) calculations are presented in Figure 5A. The principal spectral shape is a negative/positive bisignated signal that is seen to reproduce the one found in the experiment for p-HTA-D-Tyr. Results for these simple model systems thus demonstrate that single-molecule chiral deformations of the thiophene backbone can in principle produce significant ICD signals but it does not address the effects of dynamics and conformational averaging. Next, we therefore altered the dihedral angles into the forms of *trans* (T), *cis*-minus (M), and *cis*-plus (P). From this conformational study presented in Figure 5B, we concluded that the two innermost dihedral angles are of dominating importance for the CD responses of the system. It is thus well motivated to adopt a more concise categorization and presentation based on these two key dihedral angles, and the MM and PP conformational classes are identified as the most important ones. However, it is clear that for these model systems, molecular dynamics would give rise to equal populations of MM and PP conformations with a vanishing CD signal as a result, so population statistics of the chiral ligands must be introduced.

We performed an MD simulation for p-HTA-D-Tyr and analyzed the conformational variations of the thiophene backbone. The detailed statistics of the two dihedral angles around the central rings for the full trajectories as well as for a selection of 300 snapshots are provided in the SI. In light of the discussion above, we focus on the *cis* conformers and it can then be observed that the MM conformers are about twice as probable as the PP ones, showing population statistics of 9.3% and 4.3%, respectively. Together, the PM and MP conformers occupy about 8.6%. This observed difference in population statistics between the MM and PP conformer classes is very interesting as it indicates that an appreciable ICD could be observed also without dye-aggregation and also be the root cause of the experimentally observed ICD signals for p-HTA-D-Tyr.

From the MD simulations, we extracted 300 representative snapshots and determined the corresponding CD spectra. In Figure 5C, we show the spectra for each of the conformational classes, normalized by the number of snapshots, and X thus denotes that spectral summations are performed for all the conformations with different outermost dihedral angles. It is apparent and also expected from the model-system analysis, that the signal responses from the enantiomeric conformer classes XMMX and XPPX are much stronger than the responses from any of the others. The corresponding averaged CD spectrum for all 300 snapshots of a single molecule is presented in Figure 5D (blue solid line). A distinct negative/positive bisignated band is observed in the region between 300 to 450 nm, which stands in qualitative agreement with experiment.

Finally, it remains to investigate the effects on the ICD originating from intermolecular interactions upon aggregation in solution. We performed MD simulation on systems with 4, 8,12, 16, 24, and 48 chromophores under aqueous conditions. We could not observe any ordered chromophore arrangements but rather clumps of p-HTA-D-Tyr molecules with centralized thiophene backbones in π-π and herring-bone interaction patterns and tyrosine moieties at the peripheries. An illustrative aggregate structure is provided in Figure 5D. This molecular organization is in agreement with the hydrophobicity of the thiophene backbone and hydrophilicity of the tyrosine moiety. In order to address the CD spectra of the aggregate structures, we were for reasons of computational cost forced to adopt the

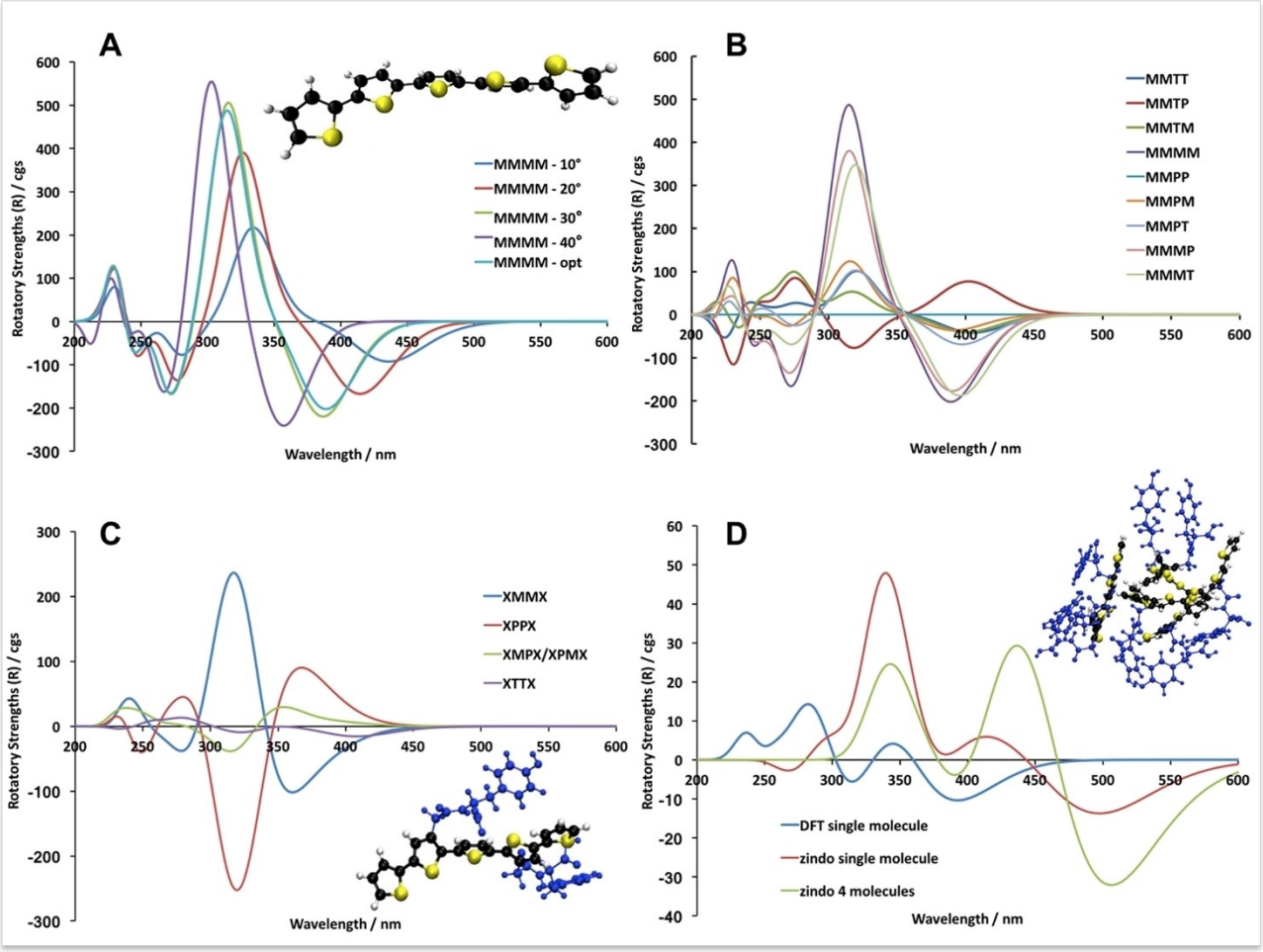

Figure 5. A) ICD calculated at the CAMB3LYP/6-31 + G(d) level of theory for MMMM conformers of pentathiophene. **B)** ICD calculated at the CAMB3LYP/6-31 + G(d) level of theory for different conformers of pentathiophene **C)** Average ICD calculated at the CAMB3LYP/6-31 + G(d) level of theory for different categories of conformers extracted from the MD trajectory. **D)** Average ICD calculated for the full trajectory of a single molecule at the CAMB3LYP/6-31 + G(d) and ZINDO level of theory and average ICD spectra for 100 snapshots of a cluster of 4 molecules at the ZINDO level of theory.

semi-empirical ZINDO approach. We benchmarked this more approximate method at the single molecule level by repeating the calculation of the averaged spectrum for the 300 snapshots. The resulting ZINDO spectrum is shown in Figure 5D (red solid line) and, aside from a 100 nm red-shift, the low-energy, bisignated, band well reproduces that of the TD-DFT spectrum. The spectral shift is not crucial for the sake of the argument and it is also a well-known systematic error built into this semi-empirical method. More importantly, the use of the ZINDO approach allows us to determine the CD spectra of the aggregates, in which case we can also expect a favorable error cancellation as to provide a reliable trend estimate. For the system composed of four molecules, the averaged CD spectrum is presented in Figure 5D (green solid line). This spectrum is also normalized with respect to the number of molecules as to be able to compare intensities against the single-molecule spectrum. We can note a general increase of the intensity as well as a small red-shift in the spectrum of the aggregate as compared to that of the single molecule. In particular, the intensity of the positive band in the ZINDO spectral region of 400–450 nm becomes quite drastically enhanced by intermolecular interactions and the resulting band profile shows a convincing qualitative agreement with the experimental spectrum for p-HTA-D-Tyr. We are led to conclude that the microscopic origin of the observed ICD under acidic conditions are rooted in the excess of MM conformer populations but enhanced by the intermolecular chromophore interactions in the formed aggregates.

2.4. Fluorescence Anisotropy Decay

By controlling the polarization state of the excitation and emission in the TC-SPC measurements, one can record the time-resolved fluorescence anisotropy, a well-known technique to monitor molecular rotation diffusion.[42] This technique is widely used to study protein complexes and interactions between proteins that alter their hydrodynamic volume. A feature of the time-resolved anisotropy is that it is difficult to accurately monitor rotational correlation times longer than the

fluorescence decay time. However, the start of the anisotropic decay can anyway give a clear evidence if a fluorescent labelled molecular complex is much larger than the non-complexed molecule as shown for e.g., amyloid aggregates.[43,44] Herein, anisotropy decay was employed to examine if the oligothiophene enantiomers were more prone to aggregation, at low concentrations (5 μM) in acidic or alkaline conditions. In 20 mM NaOH, all enantiomers displayed well-defined decays in the range 400 ps to 1 ns with the longest rotational decay time (θ) for p-FTAA-L-Tyr and p-FTAA-D-Tyr and the shortest time for the p-HTA-L-Tyr and p-HTA-D-Tyr (Figure 6, right panels). Under acidic conditions all enantiomers showed a considerably longer rotational correlation time compared to the ones obtained in 20 mM NaOH, suggesting that protonation of the anionic side chain functionalities induces aggregation of the oligothiophenes (Figure 6, left panel). The fluorescence decay time was not long enough to resolve their precise values, but anyway clearly indicated some reasonable lower limit of the size of complexes in each case. Moreover, the onset of the anisotropy at $t=0$, manifested as the r_0 value, is an order parameter indicating the angle between the excitation and emission transition dipole moments; this value cannot exceed 0.4, meaning that the excitation and emission dipole moments are parallel.[42] In all of the oligothiophene variants the r_0 was approximately 0.3 when well dissolved at the higher pH, whereas at the lower pH this value was altered (Figure 6). Thus, under acidic conditions, one might expect that the excitation and/or the emission dipoles have changed their relative directions as a result of the aggregation, comparing with the anisotropy and r_0 value of the well solvated molecule in 20 mM NaOH. This is particularly evident for p-FTA-L-Tyr and p-FTA-D-Tyr that showed increased decay-time in addition to a substantial red-shift of the emission (as discussed above). Hence, this observation further corroborates that the oligothiophene moieties are more planar in these particular aggregates.

2.5. Dynamic Light Scattering

To further investigate if the pentameric oligothiophenes go through a pH dependent structural organization, dynamic light scattering (DLS) measurements were performed in 20 mM HCl and 20 mM NaOH. When exposed to an acidic environment all ligands displayed longer lag times in the autocorrelation function compared to when exposed to alkaline conditions (Figure 7). This behavior can be attributed to a decrease in solution dynamics, indicating formation of larger structures in

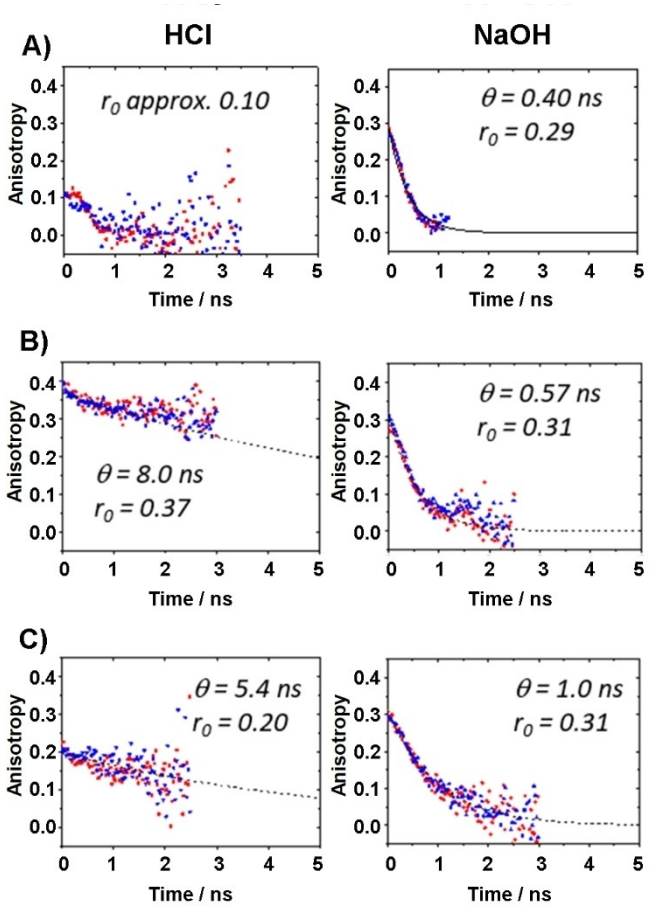

Figure 6. Time-resolved (TC-SPC) anisotropy decays of the two enantiomers of A) p-HTA-Tyr B) pFTA-Tyr and C) p-FTTA-Tyr. All samples 5 μM for D- (red) and L-type (blue) enantiomers. Left panels are at basic condition (20 mM NaOH) and right panels at acidic condition (20 mM HCl). Excitation and emission wavelengths as in the fluorescence decay measurements presented in Figure 3. The dashed curve is a mono-exponential decay with rotational lifetime, θ, as indicated in the inset and r_0, the value at $t=0$.

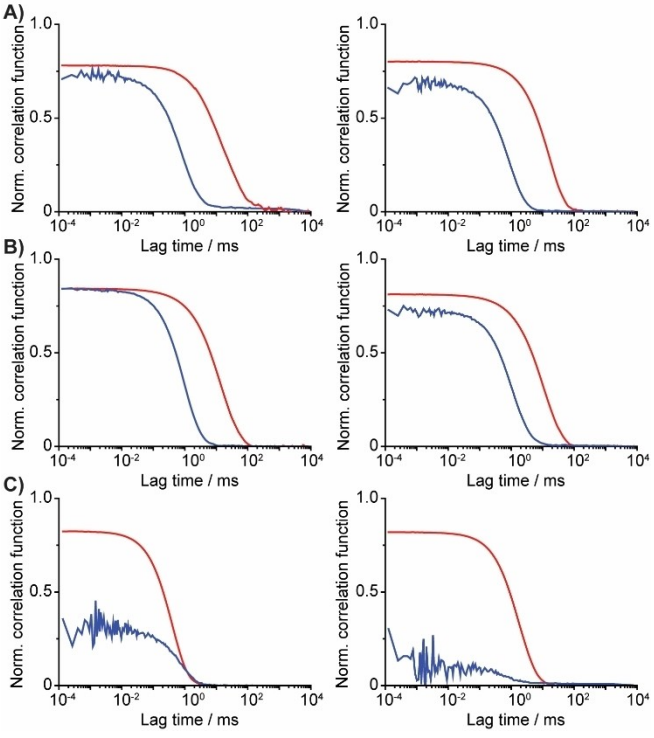

Figure 7. Correlation functions recorded by dynamic light scattering (DLS) of the pentameric oligothiophenes. A) Correlation function of 50 μM p-HTA-L-Tyr (left panel) or 50 μM p-HTA-D-Tyr (right panel) in 20 mM NaOH (blue) or 20 mM HCl (red). **B)** Correlation functions of 50 μM p-FTA-L-Tyr (left panel) or 50 μM p-FTA-D-Tyr (right panel) in 20 mM NaOH (blue) or 20 mM HCl (red). **C)** Correlation functions of 50 μM p-FTAA-L-Tyr (left panel) or 50 μM p-FTAA-D-Tyr (right panel) in 20 mM NaOH (blue) or 20 mM HCl (red).

20 mM HCl. The protonation of the carboxylic groups is hence beneficial for the self-assembly process. Both enantiomers of p-HTA-Tyr and p-FTA-Tyr formed similar sized structures in acidic conditions (Figure 7A and B), whereas both enantiomers of p-FTAA-Tyr appears to be more solubilized in the same conditions (Figure 7C). Thus, the position of the tyrosine functionality in the pentameric thiophene backbone greatly affects the organization within the structures, where a tyrosine substituent in the α-position of the conjugated oligothiophene appears to have a negative impact on the π-stacking, leading to smaller structures. In alkaline conditions both enantiomers of p-HTA-Tyr and p-FTA-Tyr form smaller structures compared to acidic conditions and both enantiomers of p-FTAA-Tyr appear to be completely solubilized, producing very weak intensities in the correlation functions (Figure 7C). Overall, DLS measurements confirmed that protonation of carboxylic moieties promotes π-stacked self-assembled aggregates and that alkaline conditions produces smaller aggregates which is in line with observations from the photo-physical characterization as well as the anisotropy measurements.

2.6. Structural Characterization of the Oligothiophenes

To elucidate the ultrastructure of the aggregated assemblies formed in acidic conditions, samples were next studied by transmission electron microscopy (Figure 8). Both enantiomers of p-HTA-Tyr displayed long fibers, 6–17 nm wide, with a tendency for lateral stacking and aggregation (Figure 8A), whereas the enantiomers of p-FTA-Tyr showed aggregates of short fibers, 6–12 nm wide (Figure 8B). Hence, oligothiophenes having tyrosine in the β-positions of distinct thiophene moieties formed fibrillar structures and longer fibrils were achieved for oligothiophenes lacking the carboxylate functionalities at the terminal α-positions of the pentameric thiophene backbone. In contrast, the enantiomers functionalized with tyrosine substituents at the terminal α-positions of the pentameric thiophene backbone, p-FTAA-L-Tyr and p-FTAA-D-Tyr showed small rather round clusters 10–30 nm in diameter (Figure 8C). Thus, alterations in the position of the enantiomeric moiety had a large influence on the molecular architecture of acid induced self-assembled structures.

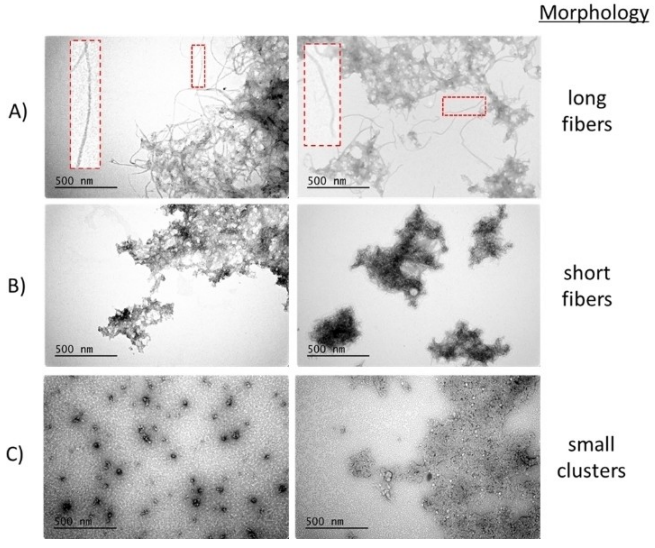

Figure 8. Transmission electron micrographs of oligothiophene self-assemblies. A) 50 μM p-HTA-L-Tyr (left panel) or 50 μM p-HTA-D-Tyr (right panel). Inset shows a zoomed-in fiber. **B)** 50 μM p-FTA-L-Tyr (left panel) or 50 μM p-FTA-D-Tyr (right panel) **C)** 50 μM p-FTAA-L-Tyr (left panel) or 50 μM p-FTAA-D-Tyr (right panel). All aggregates were formed in 20 mM HCl. Uranyl acetate 2% were used as contrast prior to microscopy.

3. Conclusions

In conclusion, anionic tyrosine-functionalized pentameric oligithiophenes were shown to exhibit pH-induced optical activity in the π–π* transition region and distinct substitution patterns of L- or D-tyrosine along the thiophene backbone governed the photophysical properties, as well as the self-assembly of the oligothiophenes. Thus, subtle variations in the position of the enantiomeric side-chain functionalities had large effects on the oligothiophenes optical characteristics as well as the molecular arrangement of the self-assembled supramolecular structures. We foresee that our findings will aid in the chemical design of chiral oligothiophenes that can be employed for different optoelectronic and biosensing applications.

Experimental Section

Full experimental details including additional characterization data and NMR spectra of new compounds, as well as supporting figures are given in the Supporting Information.

Acknowledgements

Our work was supported by the Swedish Research Council (Grants No. 2016-00748 and 2018-4343), the European Commission in the form of the ITN tiled "Computational Spectroscopy in Natural Sciences and Engineering (COSINE)" (Grant No. 765739), and the Erling Persson foundation. Computational resources was provided by the Swedish National Infrastructure for Computing (SNIC). We also acknowledge technical support from Robert Waldebring, Swedish National Forensic Centre.

Conflict of Interest

The authors declare no conflict of interest.

Keywords: oligothiophenes · chirality · induced circular dichroism · self-assembly · chiro-optical aggregates

[1] M. Lemaire, D. Delabouglise, R. Garreau, A. Guy, J. Roncali, *J. Chem. Soc. Chem. Commun.* **1988**, 658–661.

[2] D. Kotkar, V. Joshi, P. K. Ghosh, *J. Chem. Soc. Chem. Commun.* **1988**, 917–918.
[3] J. Roncali, R. Garreau, F. Delabouglise, F. Garnier, M. Lemaire, *Synth. Met.* **1989**, *28*, 341–348.
[4] M. Andersson, P. O. Ekeblad, T. Hjertberg, O. Wennerström, O. Inganäs, *Polymer* **1991**, *32*, 546–548.
[5] M. M. Bouman, E. E. Havinga, R. A. J. Janssen, E. W. Meijer, *Mol. Cryst. Liq. Cryst.* **1994**, *256*, 439–448.
[6] M. M. Bouman, E. W. Meijer, *Adv. Mater.* **1995**, *7*, 385–387.
[7] G. Bidan, S. Guillerez, V. Sorokin, *Adv. Mater.* **1996**, *8*, 157–160.
[8] F. Andreani, L. Angiolini, D. Caretta, E. Salatelli, *J. Mater. Chem.* **1998**, *8*, 1109–1111.
[9] K. P. R. Nilsson, J. Rydberg, L. Baltzer, O. Inganäs, *Proc. Natl. Acad. Sci. USA* **2003**, *100*, 10170–10174.
[10] K. P. R. Nilsson, J. Rydberg, L. Baltzer, O. Inganäs, *Proc. Natl. Acad. Sci. USA* **2004**, *101*, 11197–11202.
[11] R. Selegård, Z. Rouhbakhsh, H. Shirani, L. B. G. Johansson, P. Norman, M. Linares, D. Aili, K. P. R. Nilsson, *Macromolecules* **2017**, *50*, 7102–7110.
[12] B. M. W. Langeveld-Voss, M. M. Bouman, M. P. T. Christiaans, R. A. J. Janssen, E. W. Meijer, *Polym. Prepr.* **1996**, *37*, 499–500.
[13] B. M. W. Langeveld-Voss, R. A. J. Janssen, M. P. T. Christiaans, S. C. J. Meskers, H. P. J. M. Dekkers, E. W. Meijer, *J. Am. Chem. Soc.* **1996**, *118*, 4908–4909.
[14] B. M. W. Langeveld-Voss, M. P. T. Christiaans, R. A. J. Janssen, E. W. Meijer, *Macromolecules* **1998**, *31*, 6702–6704.
[15] B. M. W. Langeveld-Voss, R. A. J. Janssen, E. W. Meijer, *J. Mol. Struct.* **2000**, *521*, 285–301.
[16] H. Goto, E. Yashima, Y. Okamoto, *Chirality* **2000**, *12*, 396–399.
[17] E. Yashima, T. Matsushima, Y. Okamoto, *J. Am. Chem. Soc.* **1997**, *119*, 6345–6359.
[18] E. Yashima, K. Maeda, Y. Okamoto, *Nature* **1999**, *399*, 449–451.
[19] K. Maeda, S. Okada, E. Yashima, Y. Okamoto, *J. Polym. Sci., Part A: Polym. Chem.* **2001**, *39*, 3180–3189.
[20] M. Ishikawa, K. Maeda, E. Yashima, *J. Am. Chem. Soc.* **2002**, *124*, 7448–7458.
[21] K. P. R. Nilsson, M. R. Andersson, O. Inganäs, *J. Phys. Condens. Matter* **2002**, *14*, 10011–10020.
[22] K. P. R. Nilsson, J. D. M. Olsson, P. Konradsson, O. Inganäs, *Macromolecules* **2004**, *37*, 6316–6321.
[23] S. Sakurai, H. Goto, E. Yashima, *Org. Lett.* **2001**, *3*, 2379–2382.
[24] O. Henze, W. J. Feast, F. Gardebien, P. Jonkheijm, R. Lazzaroni, P. Leclere, E. W. Meijer, A. P. H. J. Schenning, *J. Am. Chem. Soc.* **2006**, *128*, 5923–5929.
[25] S. Schmid, E. Mena-Osteritz, A. Kopyshev, P. Bäuerle, *Org. Lett.* **2009**, *11*, 5098–5101.
[26] A. Digennaro, H. Wennemers, G. Joshi, S. Schmid, E. Mena-Osteriz, P. Bäuerle, *Chem. Commun.* **2013**, *49*, 10929–10931.
[27] N. A. K. Ochs, U. Lewandowska, W. Zajaczkowski, S. Corra, S. Reger, A. Herdlitschka, S. Schmid, W. Pisula, K. Mullen, P. Bäuerle, H. Wennemers, *Chem. Sci.* **2019**, *10*, 5391–5396.
[28] T. Sanji, N. Kato, M. Tanaka, *Org. Lett.* **2005**, *8*, 235–238.
[29] A. Åslund, C. J. Sigurdson, T. Klingstedt, S. Grathwohl, T. Bolmont, D. L. Dickstein, E. Glimsdal, S. Prokop, M. Lindgren, P. Konradsson, D. M. Holtzman, P. R. Hof, F. L. Heppner, S. Gandy, M. Jucker, A. Aguzzi, P. Hammarström, K. P. R. Nilsson, *ACS Chem. Biol.* **2009**, *4*, 673–684.
[30] R. A. Simon, H. Shirani, K. O. A. Åslund, M. Bäck, V. Haroutunian, S. Gandy, K. P. R. Nilsson, *Chemistry* **2014**, *20*, 12537–12543.
[31] A. Åslund, A. Herland, P. Hammarström, K. P. R. Nilsson, B. H. Jonsson, O. Inganäs, P. Konradsson, *Bioconjugate Chem.* **2007**, *18*, 1860–1868.
[32] P. Hammarström, R. Simon, S. Nyström, P. Konradsson, A. Åslund, K. P. R. Nilsson, *Biochemistry* **2010**, *49*, 6838–6845.
[33] H. Hevekerl, J. Wigenius, G. Persson, O. Inganäs, J. Widengren, *J. Phys. Chem. B.* **2014**,*118*, 5924–5933.
[34] C. Roux, M. Leclerc, *Macromolecules* **1992**, *25*, 2141–2144.
[35] B. Kim, L. Chen, J. Gong, Y. Osada, *Macromolecules* **1999**, *32*, 3964–3969.
[36] J. Kim, T. M. Swager, *Nature* **2001**, *411*, 1030–1034.
[37] J. Sjöqvist, J. Maria, R. A. Simon, M. Linares, P. Norman, K. P. R. Nilsson, M. Lindgren, *J. Phys. Chem. A.* **2014**, *118*, 9820–9827.
[38] H. Yamagata, F. C. Spano, *J. Chem. Phys.* **2012**, *136*, 184901.
[39] F. C. Spano, C. Silva, *Annu. Rev. Phys. Chem.* **2014**, *65*, 477–500.
[40] N. J. Hestand, F. C. Spano, *Chem. Rev.* **2018**, *118*, 7069–7163.
[41] L. Farouil, F. Alary, E. Bedel-Pereira, J.-L. Heully, *J. Phys. Chem. A* **2018**, *122*, 6532–6545.
[42] J. R. Lakowicz. Principles of Flourescence Spectroscopy Ch 10. 3rd Ed. Springer, ISBN 978–0-387-31278–1.
[43] M. Lindgren, P. Hammarström, *FEBS J.* **2010**, *277*, 1380–1388.
[44] J. Zhang, A. Sandberg, X. Wu, S. Nyström, M. Lindgren, P. Konradsson, P. Hammarström, *ACS Omega* **2017**, *2*, 4693–4704.

Manuscript received: May 14, 2020
Revised manuscript received: September 23, 2020